A NEUTRAL BEAM SYSTEM FOR AN IGNITION TOKAMAK*

J. Fasolo, R. Fuja, J. Jung, J. Moenich
J. Norem, W. Praeg, and H. Stevens
Argonne National Laboratory
Argonne, Illinois

Summary

We have attempted to make detailed designs of several neutral beam systems which would be applicable to a large machine, e.g., an ITR (Ignition Test Reactor), EPR (Experimental Power Reactor), or reactor. Detailed studies of beam transport to the reactor and neutron transport from the reactor have been made. We have also considered constraints imposed by the neutron radiation environment in the injectors, and the resulting shielding, radiation-damage, and maintenance problems. The effects of neutron heat loads on cryopanels and ZrAl getter panels have been considered. Design studies of power supplies, vacuum systems, bending magnets, and injector layouts are in progress and will be discussed.

Introduction

During the past year, we have considered neutral beam injector systems for an EPR and for TNS (The Next Step). In the EPR designs, 40 MW of 180 kV D^0 beam is produced by twelve injectors, with two beam lines per injector. In the TNS designs, 60 MW of 150 keV D^0 is produced by six injectors, with two beam lines per injector. Since the demands on ion sources are greater and the pumping requirements more severe for TNS (5 MW of D^0 per beam line) than for EPR (1.67 MW of D^0 per beam line), most of this discussion will be concerned with TNS injector systems.

Three design options requiring varying degrees of extrapolation beyond the state of the art for TFTR ion sources have been considered. Design 1 assumes a D^+ fraction of 75%, achieved in some present-day neutral injector ion sources, and relatively minor extrapolations in duty cycle and beam energy beyond the state of the art for TFTR ion sources. Design 2 assumes a D^+ fraction of 95%, a major extrapolation beyond the state of the art for TFTR sources. Design 3 is based on the presently remote possibility, given the current level of support, that a suitable 400 keV direct extraction D^- ion source will be developed in time to be of use for TNS. The design characteristics of the ion sources are given in Table I.

Designs 1 and 2 may be regarded as lower and upper limits to what might be achieved with sources of positive deuterium ions. Design 1, the present reference design, will be continually updated, as warranted by advances in the state of the art and by experimental determination of design parameters that can only be estimated at the present time. Design 2 represents a worthy but perhaps not quite attainable goal for further D^+ ion source development.

*Work supported by the U. S. Department of Energy.

Preliminary Layout of a $D^+ \rightarrow D^0$ Beam Line

Designs 1 and 2 both call for six injectors with two beam lines per injector. Each beam line will have a positive ion source and accelerator, followed by a double-focusing bending magnet, a neutralizer for the atomic ions, and a second bending magnet to remove atomic ions from the beam emerging from the neutralizer. Direct energy convertors will be used to recover energy from the molecular and atomic ions removed by the first and second separator magnets. Using data on the fringe fields due to the toroidal field coils, a preliminary layout of the $D^+ \rightarrow D^0$ beam line has been made and is shown in Fig. 1. For this layout, the fringe field at the exit of the neutralizer will be ~ 0.067 T. It is assumed that the volumes occupied by the D^+, D_2^+ and D_3^+ beams and the two direct convertors are shielded from stray magnetic fields but the problem of shielding these volumes without interfering with pumping and with the magnetic fields in the reactor has not yet been addressed.

For the ion sources of Designs 1 and 2, curved grids will be used in the source and accelerator to produce a convex plasma sheath and a diverging ion beam composed of diverging beamlets. The first, double-focusing bending magnet will convert the D^+ component of this diverging beam into a converging beam. Electron attachment in the neutralizer will convert about 31% of this ion beam into a converging D^0 beam which goes through a waist before it reaches the first wall of the reactor. The location of this waist and the beam size at the first wall are determined by the beam emittance, the initial beam divergence, and the bending angle of the D^+ beam. The dependence on bending angle is shown in Fig. 2 for Design 1.

D_2 gas is fed into the middle of the neutralizer at the rate of q_N torr-ℓ/s. A fraction, α of this gas flows toward the first bending magnet; the remainder, flows toward the reactor. To minimize these gas flows, the neutralizer will be tapered to follow the converging ion and neutral beams. There is a trade-off between reduced beam size at the first wall and increased neutralizer size (and gas flow) as the D^+ bending angle is reduced from 90° to 72° (see Fig. 2).

D^+, D^0 Beam Transport

For a given ion source and specified neutral beam power and energy, perhaps the most important parameters of a neutral beam injector system are the beam half-widths as functions of distance along the beam axis. They determine the sizes of neutralizers, beam ducts, and first wall penetrations (see Fig. 2). They also determine neutralizer gas loads, and, thus, gas line densities, beam losses, and neutral injector efficiencies. (Pumping speed in the magnet region is conductance limited to a value that will not permit

arbitrary reduction in pressure and beam loss for a given gas load; as the gas load increases, losses increase.) Beam transport will be discussed briefly here and in more detail elsewhere in these proceedings.[1]

Most of the transport calculations have been made by assuming that the bounding curves of the transverse (x, x'; z, z') phase space areas of the beam emerging from the accelerator are or can be approximated by an ellipse whose area is given by

$$\epsilon = \frac{\text{phase space area}}{\pi} = \omega_0 y_{0\ max} \quad (y = x \text{ or } z) \quad (1)$$

where ϵ is the emittance, ω_0 is the maximum divergence of the on-axis beam, and $y_{0\ max}$ is the half-width of the beam; the subscript 0 refers to the exit grid of the accelerator.

Equation 1 gives the correct emittance for each of the beamlets emerging from a multiaperture accelerator exit grid; however, the phase space envelope that encompasses the entire beam from a multiaperture exit grid is a parallelogram and the emittance of the beam is

$$\epsilon = \frac{\text{phase space area}}{\pi} = \frac{4}{\pi} \omega_0 y_{0\ max} \quad (y = x \text{ or } z) \quad (2)$$

It is generally assumed that the density of particles in the phase space area between the parallelogram of Eq. 2 and the inscribed ellipse of Eq. 1 is small and that this area contains a negligibly small fraction of the entire beam. This assumption has made us a bit uneasy; we have, therefore, defined a new "effective" phase space ellipse that contains a larger fraction of the beam by letting

$$\omega_0 \rightarrow (4/\pi)\, \omega_0 \quad (3)$$

$$\beta_0 = y_{0\ max}/\omega_0 \rightarrow \beta_0 = y_{0\ max}/(4/\pi)\, \omega_0 \quad (4)$$

where β_0 is the initial value of an ellipse parameter β; in terms of β and ϵ, the beam size at any distance from the source is given by

$$y_{max} = (\beta\epsilon)^{1/2} \quad (5)$$

Beam sizes calculated by using Eq. 5 with $\epsilon = \omega_0 y_{0\ max}$ (Case I), $\epsilon = (4/\pi)\, \omega_0 y_{0\ max}$ (Case II), and single-particle point-to-point geometrical transport calculations (Case III) are given in Table II for TNS Design 1. We are left with the problem of whether we should try to squeeze the last possible particle through the neutralizer by designing it to accommodate the beam sizes of Case III or let it scrape off a (presumably) small fraction of the beam and design it for Case I or Case II beam sizes. Numerical studies not yet underway are expected to give reasonable estimates of the amounts of beam scraped off in the Case I and Case II designs. Trade-off studies to determine the best option will then be possible. If scrape-off losses are found to be excessive in the Case I and Case II designs and the losses due to charge changing and dissociative collisions in the gas streaming from the neutralizer are also found to be excessively high in the Case III design, it will be necessary to reduce beam sizes by increasing the number of injectors and ion sources.

D^+ neutral beam injector design calculations (beam sizes, gas flows, beam losses, and efficiencies using the geometrical approach of Case III have not yet been completed for Design 1 of Table I, nor have they been begun for Design 2.

Design 3

Design 3, for a D^- TNS neutral beam injector system, calls for six injectors with two beam lines per injector. Each beam line will have a direct-extraction D^- ion source, with the characteristics assumed in Table I, followed by a neutralizer and a bending magnet to separate D^- and D^+ ions from the D^0 beam energizing from the neutralizer; direct energy convertors will be used to recover energy from the residual D^- and D^+ beams. A layout of the D^- beam line is shown in Fig. 3.

Curved grids will be used in the source and accelerator to produce a concave plasma sheath and a converging beam of square cross section. Electron stripping in the D_2 gas neutralizer will convert ~ 59% of the D^- beam into a D^0 beam whose size at the first wall depends on the emittance of the beam and the radius of curvature of the accelerator exit grid. The accelerator and the neutralizer are separated by a 1.0 m pumping gap to reduce the pressure in the accelerator and thus to minimize beam energy spread due to premature neutralization and grid loading due to ionization of gas in the accelerator. The Chamber I pressure is 1×10^{-4} torr and the pressure in Chamber II is 1×10^{-5} torr. Design 3 is summarized and compared with Designs 1 and 2 in Table III. Power and gas flow models for Designs 1, 2, and 3 are discussed in Reference 1.

Bending Magnet Design

A preliminary design of the bending magnet between the ion source and neutralizer (Fig. 1) has been completed. The constraints on this magnet are (1) bending radius r = 1.5 m, (2) clear aperture 0.5 m x 0.5 m, (3) field index, $n = \frac{R}{B}\frac{dB}{dR} = 0.5$, and (4) the magnet must be as open as possible for pumping, particularly along its outer circumference. Two approaches can be followed, shaping the pole face of the magnet, which results in large magnets, or pole face windings, which we have used. The resulting magnet (Fig. 4) uses currents along the boundaries of the beam region to define the magnetic field, and an iron return yoke to minimize the resulting fringe field. Current ratios of roughly (A: B: C = 4: -1: -3) give the desired field properties. The low field produced in this magnet (~ 500 G) does not require a massive iron yoke. Thus the pole faces and current carrying conductors could contain gaps which would provide a good conductance for vacuum pumping.

Neutral Beam Pumping

Two options for pumping have been considered; cryopumps and zirconium aluminum getter pumps.

Cryopumps

The refrigerant needs for neutral beam pumping are given in Table IV. Helium requirements are given in terms of liters of liquid nitrogen. The table reflects the requirements for one hour of operation of one injector. The 173 m^2 of cryopanel in each injector will operate at 4.2° K and will be shielded on both sides by 20° K panels. The 20° panels in turn will be shielded by 77° K panels.

The thermal load due to the neutron flux and the heat input from the gas load are calculated on a 75% duty cycle. Initial operation planned for a 10% duty cycle will reduce these two values by a factor of 7.5.

If the energy from the loss of beam in each injector were deposited on the pumping panel and its shields, the refrigerant requirements would increase by an enormous factor. It is, however, presumed that stray beam can be intercepted and cooled on strategically placed dumps. With this presumption, thermal loading from the neutron flux places the greatest demand upon the refrigeration. This factor alone enhances the desirability of using zirconium-aluminum getter panels for pumping the neutral beams.

Zirconium-Aluminum Pumps

Zirconium-aluminum getter panels develop high pumping speeds for active gases and especially for H_2. The panels provide a well-defined trapping volume of the gas, which is important in handling tritium, and they can be located as near to the gas source as possible. Operating experience with a zirconium-aluminum pump in the vicinity of a fission reactor core for three years shows satisfactory operation in neutron flux densities greater than expected in the vicinity of the neutral beams. Furthermore, thermal loading should have no adverse effects on performance since zirconium-aluminum pumps are normally run at temperatures of the order of 400° C to maintain active and efficient pumping surfaces in the presence of contaminants. Their disadvantages include the inability to desorb the active gases other than hydrogen when reactivated; extremely low pumping capacity for methane; and inability to pump the inert gases. For each injector, 115 m^2 of zirconium-aluminum getter panel will be required to realize the required pumping speed for deuterium.

Cryopanels would probably last as long as the life of the reactor. Zirconium-aluminum getter panels, on the other hand, have a limited life, the length of which is dependent upon the percentage of impurities, such as O_2, CO, and N_2, in the hydrogen. In Table V is some comparative data per injector, including lifetime and regeneration time, based on a 5 s injection period during each cycle.

The lifetime of the zirconium-aluminum panels is given in terms of either 1% O_2, CO, or N_2 contaminations. In practice, the neutralizer gas and fuel mixtures should have much lower contamination levels than we have assumed, making the zirconium-aluminum panel lifetime comparable to the (~ 5 years) life of the reactor.

It may be necessary to use cryopumps with the zirconium-aluminum panels to eliminate gases not pumped or poorly pumped by the panels. These cryopumps would be appendage pumps, however, and would represent, at most, a few percent of the total pumping. The combination of zirconium-aluminum panels and cryopumps still reflects a savings in initial investment and operating costs over the use of cryopumping only.

Regeneration

Table V reflects the need to regenerate the pumps under either mode of pumping. Unless provided for, regeneration would interrupt neutral beam operation. One way to avoid this would be to double the required amount of pumping panel and provide a means for isolating each half in turn when regeneration is necessary. The problem of providing reasonably vacuum tight valving to isolate hundreds of square meters of pumping panels appears staggering both in cost and complexity. If space is available, a very promising solution would be to provide one or two spare injectors. The spare injectors provide the means for rotating each injector in turn through the regeneration phase and thus eliminate the need for doubling the panel area and for panel isolation. The mode of operation will also minimize the regeneration pumping requirements, both in hardware and capacity. In addition, the spare injectors provide redundancy for on-line failures during an experiment.

Costs

There should not be much difference in initial costs between cryopanels and zirconium-aluminum getter panels. Since the cryopanels must be shielded, however, it is expected that more space within the injector will be required to accommodate cryopanneling. As the zirconium-aluminum getter panels must be operated at ~ 400° C, the thermal loading from the neutron flux and neutral beam losses becomes an asset rather than a detriment to pumping. Even if all external power were used to heat the getter panels, the cost to operate them (based on $0.0191/kW h to operate the Argonne ZGS Accelerator) would be ≃ $9.50/h per injector. The power cost to operate liquifier/refrigerator equipment to supply refrigerant to the cryopanels per hour per injector would be approximately $10.50. This figure does not reflect the high initial costs of the liquifier/refrigerator equipment. Costing this equipment separately for use with the cryopanels would probably not reflect true costs since the refrigerant needs would be lumped with the requirements for the superconducting coils and the toroidal system cryopumps, and all would be supplied from the same source.

Power Supply for Neutral Beam Source

The power system's composed of three major components:

1. A superconducting inductor which accumulates and stores the pulsed energy. This isolates the pulsed load from the utility grid.[2]

2. An invertor to generate 3-phase high-frequency power for a switched high voltage (HV) rectifier.[3]

3. A saturated time delay transformer (STDT) and a longitudinal reactor (LR) which in conjection with spark gaps and discharge resistors, protect the source during spark-down faults.[4]

Figure 5 is a diagram of the power supply system. It draws pulse energy from the superconducting energy storage inductor L_0 which is charged from the 60 Hz line between pulses. A dc/ac/dc convertor provides precisely regulated dc power for high-frequency invertors. These invertors feed a summing transformer producing 3-phase, 12.5 kHz power. This power is filtered and applied through 3-phase solid state ac switches to an HV rectifier system. The HV output leads are connected to the ion source through an STDT.

In the event of a spark in the source, the STDT prevents appreciable energy transfer into the spark. The STDT immediately initiates removal of the ac input power to the HV rectifier and discharge of the energy stored in capacitor C_2 (the capacitance to ground of the arc and filament power supplies) which is discharged into R_2 via spark gap G_2. Reactors LR limit the discharge of C_2 into the source to tolerable values.

Capacitor C_1 is discharged into R_1 via spark gap G_1 after a gap time delay (GTD) which is longer than the time required to deenergize the HV rectifier. In case the ac switches malfunction, a crowbar time delay (CTD) shorts the ac power before the delay time of the STDT has elapsed.

The neutral beam injector system provides 40 MW to the plasma for 6 5 s during startup. This requires an input power of [illegible] MW (e). Direct energy recovery of the molecular fraction of the beam provides 165 MW (e) recirculating power to the injector systems (see Fig. 1). Thus, 119 MW (e) additional power must be supplied to the injector system from the energy storage inductor.

Shielding

Nuclear analysis has been made on the duct penetration for the neutral beam injection. The reactor system modeled in the present analysis is illustrated in Fig. 6. The neutral beam port is represented by an open circular duct region that extends from the first wall through the blanket/bulk shields, passes in between a pair of toroidal-field (TF) coils, and leads to a beam injection chamber. The duct size is 4.5 m long and 0.5 m in diam. A 0.5 m thick local exterior penetration shield which consists of stainless steel (SS) or SS + 50% B_4C annular layers completely surrounds the beam duct. Radiation streaming effects through the penetrations were investigated in several regions: (1) cryopanels located parallel to the beam line inside the chamber, (2) the superconducting TF coils, and (3) the blanket/bulk shield regions in the vicinity of the beam ducts.

Figure 7 shows a nuclear heating rate along the beam duct and cryopanel walls as a function of distance from the first wall. The neutron wall loading assumed here is 1 MW/m^2. The attenuation of the nuclear heating over the 4.5 m long duct is only ~ 3 orders of magnitude. This implies that in the neighborhood of the duct wall, special considerations similar to those of the first wall/blanket must be taken in all relevant technical areas such as thermal hydraulics, material selection, and mechanical engineering. Another implication of the high radiation streaming rate through the duct is that a special component shield circumscribing the beam injector chamber is needed to prevent direct radiation streaming into the reactor building.

Cryopanels in the vacuum pumping system must be protected against a high radiation heat load in order to provide for a practical low temperature cooling capability. The present calculation shows a maximum heating of ~ 10^{-4} W/cm^3 in the cryopanels of the chamber side walls. This radiation level does not seem to cause any serious technological or economical problems relevant to the panel cooling.

Assembly

The beam injectors would be grouped in pairs, as shown in Fig. 8, with each injector having its own vacuum and power supplies, so that maintenance and conditioning of these devices could be as independent as possible. Each injector would be surrounded by a thick shield wall, and the shielding system would include some means of removing air from the high radiation environment. This is necessary because the Argon in air would become activated by the high neutron flux, complicating maintenance. Safe operation with tritium also imposes some constraints on the vacuum system of the injectors.

The cost of the injector system, exclusive of power supplies, has been estimated at about $1.8 M per pair of injectors.

References

1. J. A. Fasolo, "Power and Gas Flow Models for Monoenergetic Neutral Beam Injectors," Proc. of 7th Symposium on Engineering Problems of Fusion Research, Knoxville (1977).

2. W. R. Stacey, Jr. et al., "Tokamak Experimental Power Reactor Conceptual Design," Argonne National Laboratory, ANL/CTR/76-3 (August 1976).

3. R. L. Kustom, R. B. Wehrle, R. P. Smith, and R. E. Fuja, "Argonne National Laboratory Energy Storage and Transfer Experimental Program," Proc. of 7th Symposium on Engineering Problems of Fusion Research, Knoxville (1977).

4. W. Praeg, "Protection of Neutral Beam Accelerator Electrodes from Spark Discharges," Proc. of 7th Symposium on Engineering Problems of Fusion Research, Knoxville (1977).

TABLE 1

ION SOURCE DESIGN CHARACTERISTICS FOR THS OR EPR

	Design 1	Design 2	Design 3
Beam Energy (keV)	150 or 180	150 or 180	400
Beam Composition (D^+,D_2^+,D_3^+)	(0.75,0.18,0.07)	(0.05,0.03,0.02)	95% D^- assumed
Shape of Plasma Sheath	Convex	Convex	Concave
First Grid Transparency, τ_g	0.45	0.45	0.45
Plasma Ion Emission Current Density, j_0 (A/cm^2)	~ 0.300	~ 0.300	~ 0.178
Average Ion Beam Current Density at Last Grid, $j_+ \approx \tau_g \cdot j_0$ (A/cm^2)	0.135	0.135	0.080
Gas Efficiency, η_g	0.45	0.45	0.10
Pulse Length (s)	≥ 5	≥ 5	≥ 5

TABLE 2

SOME RESULTS OF D^+, D^0 BEAM TRANSPORT CALCULATIONS

	Case I	Case II	Case III
Initial Beam Size $2\,y_{0\,max}$ (m x m)	0.348 x 0.348	0.348 x 0.348	0.348 x 0.348
Initial Beam ½ Angle Divergence, α_0 (rad)	0.078	0.078	0.078
Maximum Initial Beamlet ½ Angle Divergence, α_0 (rad)	0.020	0.020	0.020
Emittance Definition	$\alpha_0\, y_{0\,max}$	(4/π) $\alpha_0\, y_{0\,max}$	Geometrical Transport
β_0 Definition	$y_{0\,max}/\alpha_0$	(π/4) $y_{0\,max}/\alpha_0$	Geometrical Transport
Beam Size at Neutralizer Entrance (m x m)	0.487 x 0.487	0.487 x 0.487	0.572 x 0.572
Beam Size at Neutralizer Exit (m x m)	0.339 x 0.339	0.344 x 0.344	0.472 x 0.472
Beam Size at First Wall (m x m)	0.306 x 0.306	0.390 x 0.390	0.304 x 0.304
Gas Flow Out of Neutralizer (Torr ℓ/s)	68.5	73.0	142

TABLE 3

60 MW NEUTRAL BEAM INJECTOR SYSTEM DESIGNS FOR THS

	Design 1	Design 2	Design 3
Atomic Ion	D^+	D^+	D^-
Beam Composition (D^+, D_2^+, D_3^+)	(0.75,0.18,0.07)	(0.95,0.03,0.02)	95% D^- assumed
Target for $D^\pm \rightarrow D^0$	D_2 Gas	D_2 Gas	D_2 Gas
Number of Injectors	6	6	6
Number of Ion Sources/ Injector	2	2	2
Ion Beam Current Density at Exit Grid (A/cm^2)	0.135 Avg.	0.135 Avg.	0.080 Avg.
Total Ion Beam Power, P_+ (MW)	294	222	108
Power Required to Produce the Ion Beam, $k\,P_+$ (MW)	323.5	244	119
Assumed k Value	1.1	1.1	1.1
Assumed Gas Efficiency	0.45	0.45	0.10
Gas Load/Injector (Torr ℓ/s)	252	149	46.6
Injector Pumping Speed (ℓ/s)	8.65×10^5	8.65×10^5	9.24×10^5
Zr-Al Pumping Panel Area/ Injection (m^2)	130	130	13.8
Net Power Input to Injectors (MW)	165	120	84
Electrical Power Efficiency	0.36	0.50	0.71
Pulse Length (s)	≥ 5	≥ 5	≥ 5

TABLE 4

REFRIGERANT CAPACITY PER INJECTOR PER HOUR OF OPERATION

	Watts at		Liters
	4.2 K	20 K	L/N_2
Radiation Losses	0.2	69.0	392.0
Thermal Loads (from neutron flux)[a]	454.0	1593.0	36.0
Conduction Losses	30.0	179.0	0.9
Heat Input (from gas load)	12.0	45.0	< 0.1
Totals	496.2	1886.0	434.0

TABLE 5

COMPARATIVE DATA PER INJECTOR

FOR A 5-s INJECTION PERIOD DURING EACH CYCLE

	Chamber I	Chamber II
Regeneration Frequency (days)		
Cryopanels	5.47	14.12
Zr-Al panels (Reg. at 1×10^{-5} Torr) (using both sides of panel)	8.7	22.8
Panel Lifetime (years)		
Cryopanel	Life of Reactor	
Zr-Al panel (using both sides of panel)		
17 O_2 contamination	2.2	5.7
17 CO, N_2 contamination	0.44	1.2

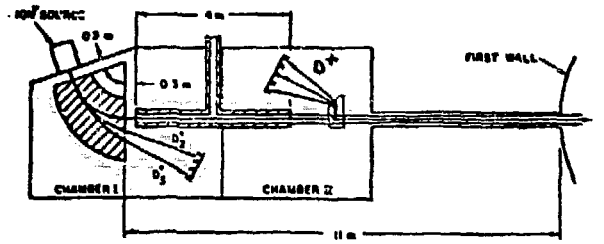

Fig. 1. Preliminary layout of a $D^+ \rightarrow D^0$ TNS beamline. The bending angle is 72°.

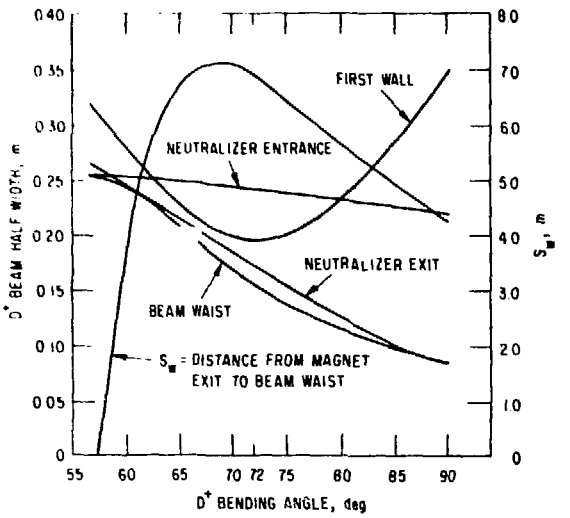

Fig. 2. Location of beam waist versus D^+ bending angle, and beam half-widths at several locations. For TNS Design I.

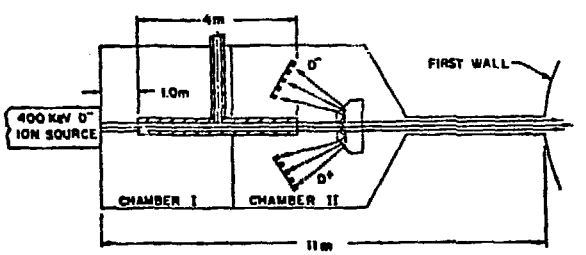

Fig. 3. Preliminary layout of a $D^- \rightarrow D^0$ TNS beam line.

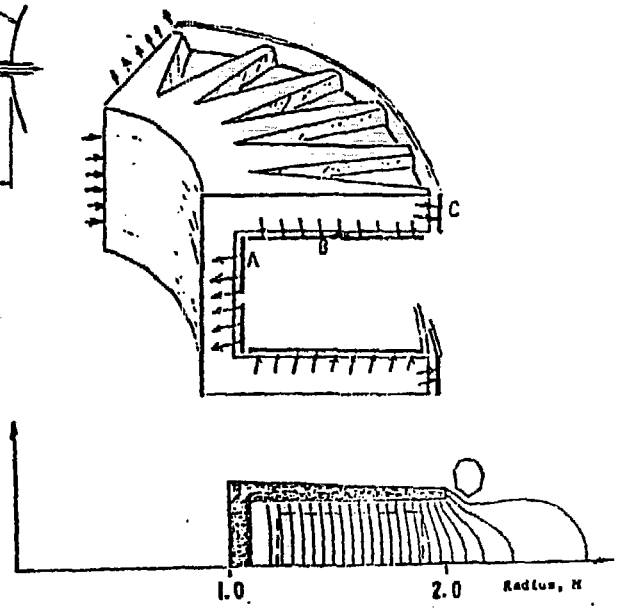

Fig. 4. Preliminary design of n = 1/2 bending magnet.

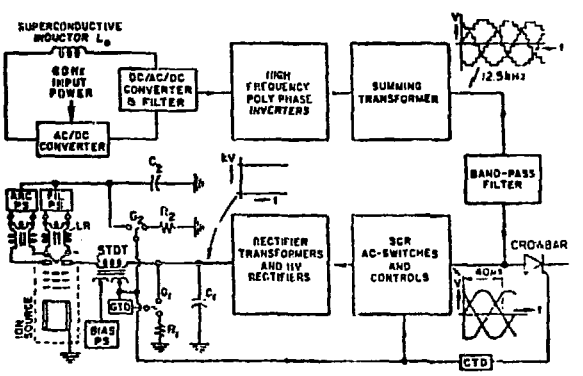

Fig. 5. Schematic of the neutral beam injector power supply system.

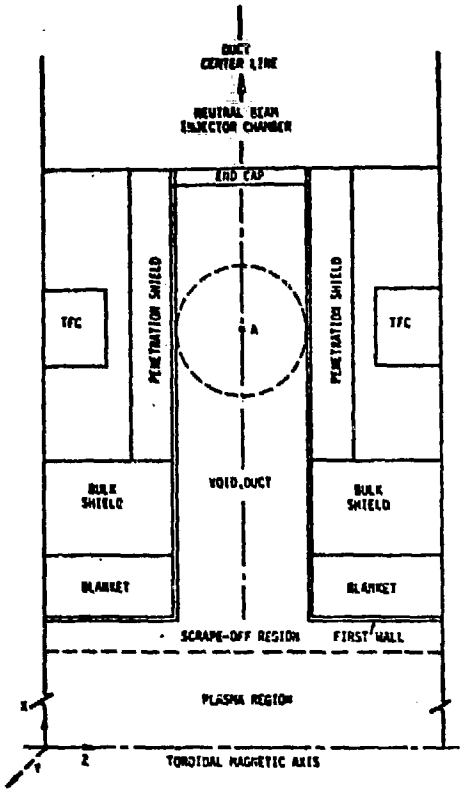

Fig. 6. Neutral beam duct model for nuclear analysis.

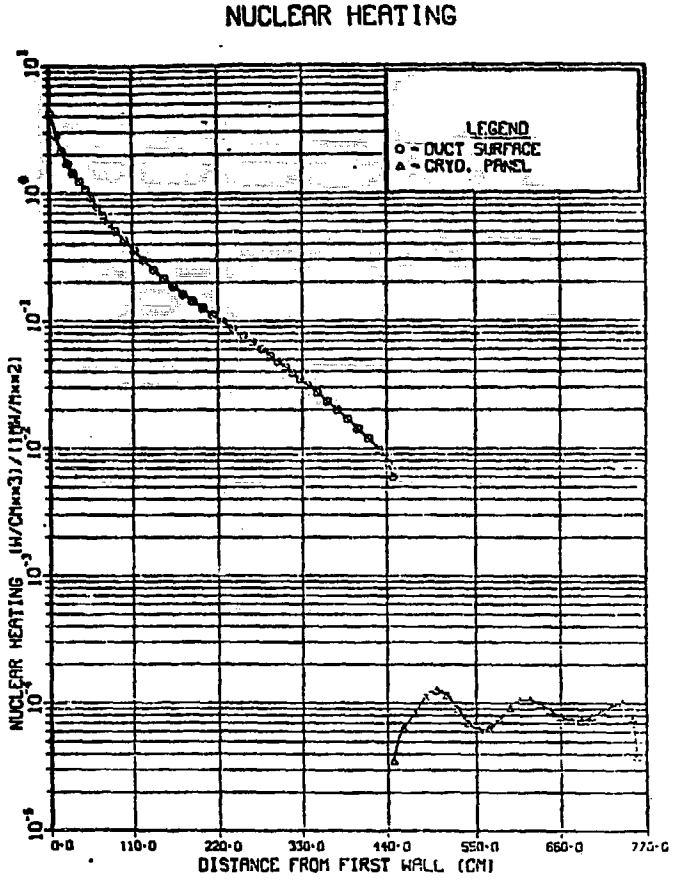

Fig. 7. Nuclear heating rates versus distance from first wall.

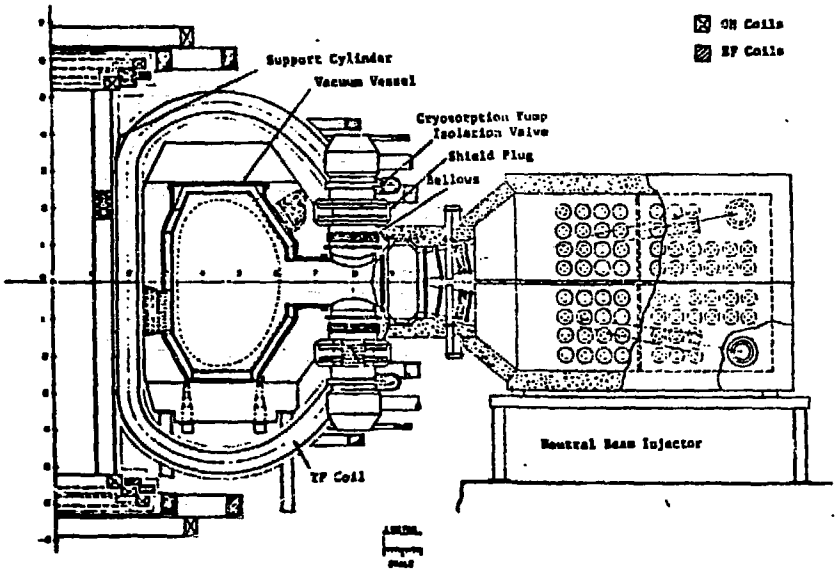

Fig. 8. Vertical elevation showing EPR torus and neutral beam design.